March 2021
ECI Project No. 4009.01

To: **Klein, DeNatale, Goldner LP**
Mr. Joseph D. Hughes, Esq.
4550 California Avenue, 2nd Floor
Bakersfield, California 93309

Westside District Water Authority
Kris Lawrence
Regulatory Compliance Manager
1405 Commercial Way, Suite 125
Bakersfield, CA. 93309

Subject: **Draft** Report Differential Interferometric Synthetic Aperture Radar (DInSAR) Study of Subsidence in the Kern County Subbasin (KCS)

Earth Consultants International (ECI) are pleased to present this report describing the scope of work, methodology, findings, and conclusions of a Differential Interferometric Synthetic Aperture Radar (DInSAR) study of the KCS. The purpose of this study was:

1. To assess the magnitude and potential drivers of land subsidence within the KCS between 2015 and 2020,
2. To assess recent DInSAR data in comparison to National Aeronautics and Space Administration/ Jet Propulsion Laboratory (NASA/JPL) subsidence data, and
3. To provide recommendations for the next steps.

DInSAR imagery for this study was obtained from Sentinel-1 radar images combined with a Short Baseline Subset (SBAS) stacking algorithm to create (1) a time series to measure subsidence and (2) for the creation of figures showing the measured average subsidence rates within the KCS) for the period April 2015 through September 2020. The project was initially intended to include radar imagery collected by the Japanese ALOS 1 & 2 satellite systems for the years between 2007 to 2011 and from 2014 to the present. Concerns about the poor quality of the raw radar images and its potential effect on data resolution prevented the use of this data.

To achieve maximum resolution ECI downloaded, processed and analyzed a total of 172 Sentinel-1 SAR images dating from May 3, 2019. This data represents the period spanning from the end of a historic stack of Sentinel-1 interferograms created by NASA/JPL through the end of September 2020. In total the DInSAR stack generated by ECI contained 526 interferograms spanning the period of interest (i.e., 2015-2020 for this current study. The DInSAR interferometric stack created in this study was combined with the NASA/JPL stack and Line-Of-Sight (LOS) velocities were generated from the combined data using a Least-Squares processor developed by ECI.

For presentation, the processed output of the two combined interferometric stacks was converted from millimeters to inches and the subsidence was classified into 13 color coded intervals ranging from 1 to >40 inches. To the extent possible ECI utilized the same color coding as those provided on the NASA/JPL figures. For reference, and to place the findings of this current study in context, the NASA/JPL subsidence figures generated from 2015-2017 InSAR data are provided herein. (Figures 1 to 5a). These are discussed further in Section 4.1 of the report.

The raw cumulative and annual displacement (i.e., subsidence) data was used to create seven transects oriented west to east (Figure 6). Figures 7 and 8 present the current study period cumulative subsidence and annual rate of subsidence, respectively. The individual transects shown on Figure 6 are presented in detail on Figures 9a through 9g. Transect A to A′ spans the Valley approximately 4.5 miles to the north of the KCS boundary. This transect serves as a point of reference and comparison to the data within the KCS. It also provides a potential basis for SGMA-required planning and project management actions with Groundwater Sustainability Agencies (GSAs) adjacent to the KCS. The six other transects (B to B′ through G to G′) cover the entirety of the KCS. To assess interferogram stack quality, point time series data were extracted at the location of 13 continuous GPS stations. Plots were created combining data for each location, using time series data from the GPS stations, the NASA/JPL stack and the DInSAR stack created for this study (Figures 10a to 10m). The point time series plots for each GPS station were utilized to ground-truth the results of the SBAS stacking process. The time series plots exhibited a robust correlation between the vertical velocities measured by the continuous GPS stations and the velocities measured by the study InSAR stacking. As a further quality check, five point time series plots (Figures 11a to 11e) were also created for locations with subsidence known to be driven by different mechanisms (i.e., groundwater extraction versus oil field activities). These plots illustrate the difference in subsidence over time associated with extraction of oil and gas, which has a nearly linear, uniform subsidence pattern versus subsidence driven by groundwater extraction, which usually has a distinctive cyclic, seasonal subsidence pattern over time. For a baseline comparison one point was also selected in a “stable area” with nearly zero subsidence over time. Figures 12 to 34 provide cumulative subsidence and annual rate of subsidence for the study period for the individual GSAs within the KCS.

The ECI subsidence maps, point time series and subsidence transects verify the general subsidence patterns identified by earlier investigations by NASA/JPL (Farr et al 2015, 2016), TRE Altamira (2019) and the statistical study of the TRE Altamira report done by Towill, Inc (2020) commissioned by DWR.

An important preliminary finding of this study is that the short time spans (e.g. 1-3 years) used in some of the previous studies are likely overestimating the subsidence in groundwater extraction areas due to the inherent variability in short- and long-term subsidence rates. The calibrated velocities along satellite LOS in this current study is between 45 to 50% of the subsidence rates previous reports described in areas with subsidence driven by groundwater extraction. That is, previous studies may have overestimated KCS groundwater extraction related subsidence by a factor of up to 50%. By way of comparison, this does not appear to be the case for areas with subsidence driven by extraction of oil and gas, where we found the subsidence rates to be the same or somewhat larger than in previous studies. The discrepancy in the subsidence data may be affected by the cyclical nature of groundwater extraction as compared to the more steady, non-cyclical, characteristics of subsidence associated with oil production. Further assessment of this phenomenon is recommended as part of KCS SGMA project management action planning.

We hope that the information presented in the following report provides you with the data you need at this time. We appreciate the opportunity to provide these services to the KCS. Should you have any questions regarding the above, please do not hesitate to contact us at your earliest convenience.

Respectfully submitted,
EARTH CONSULTANTS INTERNATIONAL, INC.
Registered Geologists, Certified Engineering Geologists and Certified Hydrogeologists

Anders Hogrelius, PG 9693
Senior Project Consultant

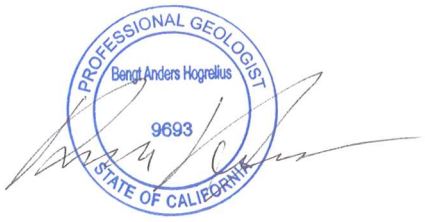

TABLE of CONTENTS

FIGURES

Draft Differential Interferometric Synthetic Aperture Radar (DInSAR)
Study of Subsidence in the Kern County Subbasin (KCS)

1.0 INTRODUCTION

1.1 PURPOSE OF THE STUDY

Earth Consultants International (ECI) conducted a ground subsidence study for the Kern County Subbasin (KCS, subbasin, or Subbasin) area using stacked satellite-based Differential Interferometry Synthetic Aperture Radar (DInSAR). The purpose of the study was:

1. To assess the magnitude and potential drivers of land subsidence within the KCS between 2015 and 2020,
2. To assess this recent DInSAR data in comparison to National Aeronautics and Space Administration/ Jet Propulsion Laboratory (NASA/JPL) subsidence data, and;
3. To provide recommendations for the next steps.

The primary objective was to provide information to KCS stakeholders which could be utilized with regard to SGMA-required planning. A secondary goal was, to the extent feasible, to differentiate between sources of subsidence and their potential impact on critical infrastructure like canals and aqueducts within the KCS.

1.2 REGULATORY AND PRACTICAL FRAMEWORK GUIDING THE STUDY

In 2014, the State passed the California Sustainable Groundwater Management Act (SGMA), a piece of legislation comprised of three separate bills, including Assembly Bill 1739, Senate Bill 1319, and Senate Bill 1168 (State Department of Water Resources, 2015). The SGMA, which went into effect on January 1, 2015, requires the formation of local Groundwater Sustainability Agencies (GSAs) whose role is to monitor and ensure that groundwater resources in the State are used and managed sustainably. As a result of the drought that California experienced during 2010 through 2016, and the increasing number of water supply users, many of the groundwater basins in central and southern California have been, and are being pumped in excess of their natural rate of replenishment with a resultant drop in the groundwater table. In some areas this in turn has led to compaction of the geologic sediments and significant land subsidence, with concomitant damage to groundwater aquifers, utilities, public infrastructure, and some natural resources such as groundwater-fed streams and springs.

Senate Bill 1168 requires, among other things, the GSAs prepare GSPs and to regularly measure and monitor the depth to groundwater in their basin and calculate the maximum amount of water that can be pumped out of the basin in a year without causing an "undesirable result." An "undesirable result" can include any of the following: 1) chronic or persistent lowering of the groundwater level, 2) significant and unreasonable reduction in groundwater storage, 3) significant and unreasonable seawater intrusion, 4) significant and unreasonable degradation of water quality, 5) significant and unreasonable land subsidence, and 6) depletions of surface water that result in significant and unreasonable adverse impacts on beneficial uses (Water Education Foundation, 2015). The focus of this current study is land subsidence and how an integrated approach utilizing both land and satellite-based technology can be economically utilized to accurately measure and model this phenomenon.

Traditionally, the monitoring of ground surface deformation has been conducted using spirit-leveling (surveying) techniques. This method is very precise but potentially costly and time-consuming. Further, the data is often spatially and temporally sparse, as measurements are made at relatively few locations, and at temporal intervals typically measured in months or years (e.g., Poland et al.,

1984). Extensometers are another method of measuring ground subsidence. These provide reliable data, but are expensive to install and maintain and, like surveying, typically provide sparse, localized data coverage.

DInSAR has been used for more than 20 years by government agencies and research institutions to assess the conditions of topographic elevation changes, to monitor groundwater basins in order to quantify potential sediment consolidation, and to monitor surface deformation resulting from the extraction and/or recharge of groundwater (for a few examples of these studies, refer to the links provided in the References Section of this report). Compared with the other direct-measurement methods briefly described above, DInSAR is considered more cost- effective, as this method can cover large areas without the need for surface access agreements and maps both the magnitude of the vertical deformation and its spatial distribution within a study area.

Provided a suitable number of satellite passes are available, DInSAR combined with a stacking algorithm can also yield changes in elevation over relatively short time intervals making it particularly useful for assessing cyclical surface changes. Finally, recent developments in the processing of interferograms to provide time-series analyses have further increased the potential value of DInSAR as a method for the monitoring of aquifers. The level of detail and broad areal coverage that DInSAR can provide make it a useful tool along with continuous GPS for local GSAs looking to adopt sustainable management plans in response to the requirements of the SGMA.

2.0 TECHNICAL BACKGROUND

2.1 DIFFERENTIAL INTERFEROMETRY SYNTHETIC APERTURE RADAR (DInSAR)

The DInSAR method relies on the processing and comparison of two Synthetic Aperture Radar (SAR) images of the same portion of the Earth's surface taken by the same satellite system on two different passes. In simple form; -in recurrent passes a satellite bounces a radar (microwave) signal off the Earth's surface and records the phase and amplitude of the reflected signal. The product resulting from the digital comparison of the phase component of two or more SAR images is called an interferogram; the resulting image illustrates and quantifies the changes in the ground surface elevation that occurred between the two satellite passes used in the analysis. The method can detect vertical changes of the ground surface of as little as 5 mm (0.2 inch) for standalone interferograms. A resolution below 5 mm can be achieved when multiple interferograms are used together with a stacking algorithm. The SAR images from the satellite platforms that ECI used for this study (discussed further below) have a surface (horizontal) pixel resolution of 25 meters (m; ~82 feet) with no space between pixels. The vertical resolution of the subsidence rates derived from this DInSAR stack is approximately 2.4mm/year or $\pm 1\sigma$ (Standard Deviation) based on comparisons with data from continuous operating GPS stations (UNAVCO and SOPAC) in the target area. For the areas with the largest subsidence this represents an error of ~1% of the annual subsidence rates.

As of September 2020, when the analysis for this study was initiated, archived satellite data from the three selected satellite systems were available for the past 10 years (2010 to 2020), as follows:

1. The Japanese Space Agency (JAXA) ALOS 1 (2006 - 2011)
2. The Japanese Space Agency (JAXA) ALOS 2 (2014 - current)
3. The European Space Agency (ESA) Sentinel-1A/B (2015 - current)

Data from all the satellite systems is available through the respective data portals for the European Space Agency (ESA) and the Japanese Space Agency (JAXA) as well as through the Alaska Satellite Facility (ASF) operated by the Geophysical Institute at the University of Alaska Fairbanks. A radar image generated by one of these satellites cannot be directly compared to an image generated by another satellite system, so the interferograms that are generated have to be based on images from the same system. The generated interferograms can be compared across satellite platforms. Data quality concerns related to the ALOS 1 & 2 systems precluded its use in the current study. This prevented extending the study period to encompass historic data for the period 2007 to 2011.

Interferometric patterns that may result from the comparison of two or more paired radar images from different time periods may be used to interpret subsurface structures defining the margins of aquifers as well as internal structures and stratigraphy, especially when combined with data from other sources like groundwater extraction records, water level data and well logs. Once a baseline is established and calibrated, yearly, biannual, or quarterly interferograms can be used as a cost-effective management tool for monitoring the conditions of the basins.

By combining the DInSAR stack from NASA/JPL with the interferometric stack generated in this study ECI identified discrepancies in the calibrated velocities along satellite LOS. The study by NASA/JPL appears to overestimate the subsidence rates for the areas with groundwater-driven subsidence by as much as 45 to 50%, though the subsidence rates for areas with subsidence driven by extraction of oil and gas are comparable between this current study and the earlier NASA/JPL data. We attribute this discrepancy to errors introduced when using linear regression on a dataset that covers a timespan that is too short (e.g. one to two years of withdrawal – recharge cycles of the aquifer) when the data contains cyclic (seasonal) changes.

Additional information on DInSAR, including the methodology used to process the data, is provided in Section 3.1 and Appendix A.

2.2 GROUND SUBSIDENCE RESULTING FROM GROUNDWATER EXTRACTION

In California, land subsidence primarily occurs as a result of groundwater extraction but can also result from tectonic activity (mountain forming and seismic events), natural consolidation of sediment, oxidation, and compaction of organic deposits, hydro compaction of moisture-deficient soil and sediments, and extraction of oil (Poland et al., 1984; Galloway and Burbey, 2011; Borchers et al., 2014). Contributing factors to subsidence caused by oil extraction activities in the KCS and their potential to impact critical infrastructure are discussed in Section 2.3 of this report.

Aquifer systems experience some degree of deformation in response to changes in hydraulic stress, which include natural (rainfall) recharge and/or artificial recharge, or withdrawals such as groundwater pumping or reinjection (Galloway and Burbey, 2011; Bawden, 2003). The seasonal cycle of discharge and recharge from unconsolidated heterogeneous aquifer systems, such as those underlying many locations in the Central and San Joaquin valleys and the Santa Clara and Antelope valleys, typically causes measurable elastic (recoverable) land subsidence and subsequent, proportionate uplift (measured in millimeters to centimeters) of the land surface. Removing water from storage in fine-grained sediments (silts and clays) interbedded in the aquifer system can cause these highly compressible sediments to compact inelastically and permanently as pore pressure is reduced. Land subsidence from inelastic (non-recoverable) compaction is a common consequence

of significant groundwater level changes that can result from development of groundwater as a resource (Borchers et al., 2014; Sneed, 2016).

There are some limitations to the use of ground surface deformation data for monitoring aquifers. Specifically, for surface subsidence to occur, there must be one or more compressible layers of sufficient thickness under static conditions below the top of the saturated zone. These layers can consist of multiple stacked or interlensing fine grained layers, or a single subregional fine grained member, such as the Corcoran Clay. Additionally, the layers need to have been dewatered during extended periods of continuous pumping. All of these factors can be found in the Central Valley. Reversible (elastic) surface deformation may occur as the pore pressure within the compressible layers cyclically rises and falls during either seasonal or other forms of alternating short-period extractions and recharge. Alternatively, if the compressible layers are dewatered due to pumping without significant recharge for an extended period of time (i.e., several years), irreversible (inelastic) surface deformation will typically occur (Bawden, 2003; Borchers et al., 2014; Orange County Water District, 2016). Monitoring of surface deformation is thus primarily a useful tool if (1) the aquifers in question contain suitable compressible layers, and (2) those layers have not been previously dewatered for an extended period of time below a depth termed the "pre-consolidation stress" (e.g., prior historical low water level). Both elastic and inelastic compaction related to groundwater extraction has and is occurring in the Central Valley. For example, a large and historically propagating subsidence bowl immediately north of the KCS is attributed to dewatering of both the Corcoran Clay and fine-grained lenses to the east beyond the extent of the Corcoran Clay. The leading edges of this bowl appears to be impacting the KCS near Delano. By way of contrast, surface elevation stability or elevation increase in the KCS is also discernable in the data, due to groundwater banking activities and direct recharge via losing streams and along mountain fronts that border the KCS.

2.3 GROUND DEFORMATION RESULTING FROM EXTRACTION OF OIL AND GAS

Subsidence caused by oil field activities can be differentiated from those of seasonal agriculture. Oil field activities by their nature are long term and constant. As such they are readily discernable on DInSAR and the pattern of subsidence generally does not exhibit variability over time. Data from this current study has confirmed this phenomenon. Examples in the KCS include the Lost Hills, Cymric, Elk Hills, and Belridge oil fields, among others.

Recent technical review studies conducted on behalf of the Westside Water Authority (WDWA) have concluded that oilfield activities in the Lost Hills Oil Field (LOHF) are a contributing factor to subsidence between mileposts 195 and 215 on the California Aqueduct. In 2018, the LHOF generated approximately 13,500 acre-feet (AF) of produced water. By way of contrast, the WDWA estimates it has historically pumped only around 3,000- 5,000 AF/year for the purpose of blending the naturally poor-quality groundwater with Aqueduct water when supplies are short. Most of its irrigation water is provided by the Aqueduct (Aquilogic 2019, 2020).

Oilfield-operator aquifer exemption application materials submitted to the State document that oil extraction causes subsurface water (aka "produced water") to move up-structure due to subsurface pressure differences. According to the WDWA study, this action can withdraw subsurface water from beneath the Aqueduct, contributing to the identified undesirable subsidence results between the above referenced mileposts. The WDWA study concluded this is particularly true for areas where the Aqueduct lies adjacent to the LHOF and/or in places where the oil field geologic structure

extends beneath the Aqueduct at depth (Aquilogic, 2020). A comparison of DWR Aqueduct subsidence profiles to oil field cross sections produced by the oil field operators showed a strong correlation between oil pumping and Aqueduct subsidence (Aquilogic, 2020). The WDWA study provides a basis for interpreting the DInSAR data generated by this current study. The DInSAR shows subsidence centered on the LHOF, which extends slightly to west and the east. Without the recent WDWA study this data could suggest a significant contribution from agricultural pumping to the aforementioned Aqueduct subsidence, as preliminarily reported by the DWR. However, the WDWA study indicates the irrigation well density within a five-mile radius of the Aqueduct is sparse in comparison to the number of oil wells in the LOHF (Aquilogic, 2020), and the DInSAR data produced in this current study has the characteristic signature of subsidence associated with oil field activities.

3.0 WORK COMPLETED AND METHODOLOGY FOLLOWED

Pursuant to our proposal dated June 18, 2020, ECI completed the tasks outlined below as part of this study. A more detailed description of the DInSAR method and data sources is provided in Section 2.1 and Appendix A.

3.1 QUALITY OF ALOS-1 & -2 DATA

Part of this study had intended to use historic ALOS-1 & -2 satellite data to supplement the more recent Sentinel-1 data. To assess data viability and quality ECI downloaded a total of 328 radar images from the Alaska Satellite Facility. All radar images were selected based on the geographic footprint of the study area to ensure that the whole target area was covered. ECI also ensured that the "Baseline Perpendicular Offset" of the images (Perpendicular offset between recurring orbits. See Appendix A) was within an acceptable range for successful InSAR processing. These images were then pre-processed and prepared for interferometric processing with the DInSAR processing package developed by Scripps Institute of Oceanography, Generic Mapping Tool Synthetic Aperture Radar (GMTSAR).

Results from the first processing attempt indicated potentially severe quality issues with both the ALOS -1 & -2 images. The parts of the images that were furthest in range from the satellite (SAR equipped satellites are always looking down at an oblique angle), were distorted. When these images were combined to form an interferogram it was apparent that many images also were offset along azimuth (flight path of the satellite orbit) likely due to poor control of the satellite's internal clock. Attempts at working around the problem by using a different DInSAR processing package, ROI_PAC developed by NASA/JPL, were unsuccessful due to the same quality problem. Further attempts at processing the ALOS data was thus abandoned as being non-viable and having unreliable quality, as both DInSAR processors failed with the same error. Therefore, in order to achieve maximum resolution, the ALOS data was not utilized for this current study.

3.2 INSAR PROCESSING OF SENTINEL-1 DATA, COMBINING AND STACKING INTERFEROGRAMS

A total of 172 Sentinel-1 radar images were downloaded from the European Space Agency and after pair-wise merging of neighboring images the resulting 86 SAR images were processed using the GMTSAR processor. The 86 SAR images were combined to produce 526 interferograms. By stacking this number of images ECI was able to correct for the effects of ambient moisture in the atmosphere on the interferometric data. The removal of the atmospheric effects (which can be substantial) due

to moisture in clouds, transpiration and fog is important for achieving data accuracy. By using multiple interferograms created from different radar images within the same interferometric dataset, it is possible to calculate, and then subtract, the atmospheric effect on all but the first and last image in the stack. The first and the last slice in the interferometric stack can for that reason contain data outliers. However, the second step of the stacking process utilizes a least-squares method on corresponding pixels in every slice of the interferometric stack to extract a map of the surface velocities along LOS from the satellite. In so doing, the potential for data outliers to affect the final result is minimized. The initial stacking and atmospheric corrections are corrected with a Short Baseline Subset (SBAS) algorithm included in the GMTSAR package.

When re-stacking the slices after calibration to tie down the interferometric stack to stable points or to calibrate the stack to deformation recorded by continuous GPS stations, ECI applied a least-squares software package to the stacked data. Following the creation of ECI's interferometric stack, this same software package was also used when combining interferometric stacks from NASA/JPL to calculate the combined displacement rates (see Section 3.4). To remove the last traces of atmospheric interference from the interferometric stack, ECI used a process where a stable point (i.e., near zero subsidence) is identified within the footprint of the satellite images. In this case we used the CORS GPS station ISLK operated by UNAVCO, which shows long-term stability because it is located far from known sources of deformation (i.e., faults and areas with subsidence or uplift). All slices in the interferometric stack were adjusted so the value of the pixels corresponding to the location of the stable reference point is equal to zero (or in general, matching the displacement of the GPS station). The interferometric stack can then be re-processed with the least-squares software to generate maps where the displacement rates are calibrated (i.e., tied to GPS data).

3.3 Combining and post-processing the Sentinel-1 stack with NASA/JPL data

Due to the relatively short time span of the stack (i.e., April 2015 – May 2019) acquired from NASA/JPL and the short time span of the interferometric stack generated in this study (i.e., May 2019 to September 2020), it was determined that a better option was to create a combined stack spanning the full five-year period between April 1, 2015 through September 30, 2020. This was done by co-registering the ECI stack with a subset of the NASA/JPL stack and then adjusting it by adding the last slice in the NASA/JPL stack to all following slices in the ECI stack. This was possible because there was a small time overlap between the two stacks, and because one slice near the end of the NASA/JPL stack has a date matching the first slice in the ECI stack. With this process completed, we ran the merged stack through a least-squares processor and generated a velocity map for the complete period between 2015 and 2020. The ECI least squares processor also outputs a map of the R^2 ("goodness of fit") values which allows us to filter out areas where the correlation is low between the pixel values in the stack and the resulting velocity. For the maps in this report, we used an R^2 value as 0.67 as the threshold, and everything with a lower value was filtered out.

3.4 Correlating DInSAR velocities with permanent GPS (GNSS) stations

For quality control and for comparison to the NASA/JPL data we used 13 continuous GPS stations for which we downloaded available time-series data. Time series for these locations were then extracted from the corresponding location in the two DInSAR stacks and data from all three sources were then plotted together and examined. The trends of the three graphs, GNSS, NASA/JPL- and ECI DInSAR time series all show matching patterns in addition to the slopes of the DInSAR graphs matching recorded GPS data. There is too much noise (i.e., inherent atmospheric and ionospheric noise) in the NASA/JPL DInSAR time-series data to be able to recognize the fine seasonal changes

in subsidence seen in the GPS data, but overall the trend and slope of the two patterns match. With the SBAS algorithm used by ECI on the Sentinel-1 data for the period between May 3, 2019 and September 30, 2020, the fine seasonal deformation patterns match the GPS data well, showing a robust correlation between DInSAR and GPS measurements. Examples for these two conditions are presented on Figures, 10a, 10b, 10d ,10e and 10h respectively.

3.5 Extraction of transects and point time series

As part of this study, we extracted seven west-to-east transects (showing annual rates and cumulative displacement), roughly equally spaced from the northern to the southern boundaries of the KCS. The placement of the transects cover critical infrastructure such as the Aqueduct and oil fields (Figure 6). For orientation purposes, markers showing the location of canals, major roads and oil fields were inserted into the transects. Extraction of transects and raster calculations for conversion between millimeters and inches were done with QGIS and the resulting text files with the cross sections were subsequently plotted with the Generic Mapping Tools (GMT). A similar technique was used when extracting data from the interferometric stacks (See the previous section 3.4). We used GMT to extract the deformation values stored in the pixels at chosen geographic locations in the raster files that makes up the interferometric stack, transferring the values to text files. These files were then plotted in GMT together with data from the continuously operating GPS stations. To illustrate the difference in subsidence patterns over time in areas with extraction of oil and gas, versus areas with groundwater extraction, five point-time series were also extracted from the stacked DInSAR data. Two point-time series from each type of area were generated with an additional point series generated in a stable area with no known subsidence.

4.0 FINDINGS AND DISCUSSION

4.1 SUBSIDENCE WITHIN THE KERN COUNTY SUBBASIN

The preliminary result of this current DInSAR study found that subsidence rates associated with seasonal groundwater extraction within the KCS over the period 2015 to 2020 are likely 45 to 50% lower than estimated by the NASA/JPL. This is because of previous studies assessed shorter time intervals that can be subject to greater variability in the raw InSAR data due to seasonal changes in the subsidence rate. Based on data from NASA/JPL (*Progress Report: Subsidence in California, 2015, 2017*), subsidence rates of between 8 and 9 inches per year are estimated for the most rapidly subsiding area at the northern border of the KCS west of Delano. Based on the longer time series utilized in this study, a subsidence rate of 2 to 3 inches per year is estimated for the same area. Similarly, the maximum subsidence rate for groundwater extraction in the subsidence bowl south of Bakersfield is estimated to be 6 to 7 inches per year for the previous shorter NASA/JPL data time series. The data for this current study estimates average subsidence rates for this same area as between 3 to 4 inches per year. A likely cause for these discrepancies lies in the changes in subsidence over time due the cyclical pumping and recharge of underlying aquifers and more long-term effects such as drought conditions. These patterns are very clear when looking at the DInSAR time series for the two GNSS stations BKR1 and BKR2, where both short, cyclical, and long-term effects are visible (Figures 10d and 10e).

We have also observed that the noise evident in the stacked data from NASA/JPL may cause problems especially when looking at shorter time spans. Though the long-term subsidence rates that can be calculated from their stacked data closely matches the subsidence rates as measured by the continuous GPS stations in the region, this noise makes it impossible to study the finer seasonal fluctuations. Furthermore, this noise significantly reduces the correlation and introduces an

uncertainty in the calculated subsidence rates. Some of these effects are evident in many of the NASA/JPL figures from previous studies and present as patches of white (i.e. no color) in areas of identified groundwater extraction induced subsidence.

For the estimated subsidence rates, it is important to note that these velocities are calculated over a longer period of time, and that these will be different from the cumulative subsidence over the same time period. This is due to the large variability in subsidence rate over time, something which is evened out when doing a least-squares regression of the subsidence to calculate the average subsidence rate.

It is also important to note here that although subsidence is generally thought of as a purely vertical process, there are significant horizontal geo-mechanical stresses associated with land subsidence that are often overlooked. These stresses are known to increase over distance from the center of the source of the subsidence, reaching a maximum near the hinge line of the depression and can have deleterious consequences for linear infrastructure such as aqueducts, pipelines, canals, and rail tracks. A separate 3-dimensional analysis of the horizontal stress patterns and their potential impact on critical infrastructure in the KCS is needed for a more complete understanding of potential undesirable results.

The five identified areas of interest (AOIs) for subsidence are presented on Figure **5a**. These areas were previously identified based on NASA/JPL data for the periods 2015 to 2016 and 2015 to 2017 (i.e., 2015-2017). Below is a comparative update based on this current study utilizing DInSAR data from April 2015 to September 2020.

Friant-Kern Canal (AOI 1)

This AOI was rated by the GSAs in the KCS as high priority for monitoring between Mileposts 120 to 130, east-northeast of the City of McFarland (Figure 5a). At times, previous InSAR monitoring has detected up to 5 inches per year of subsidence in areas surrounding this segment of the Friant-Kern Canal. The current study indicates that the rate of annual subsidence in this AOI averages between 2 and 3 inches (**Figure 8**).

California Aqueduct Mileposts 196 to 215 (AOI 2)

This AOI was identified as high priority by the GSAs in the KCS. It consists of a segment of the Aqueduct where an embankment failure occurred at Milepost 208 in June of 2011 (**Figure 5a**). While additional studies to assess and monitor subsidence in this AOI are planned, a separate study by WDWA in 2019 and early 2020 has identified LOHF activities as a contributing factor to the identified subsidence (see Section 2.3). This current study shows the subsidence along this segment of the Aqueduct displays the characteristics of oil field activities, and that the LHOF is isolated by areas of generally lower annual subsidence, suggesting that agricultural groundwater extraction is minimal in this area. (**Figure 8**).

Friant-Kern Canal Mileposts 130 to 137 (AOI 3)

This AOI was identified as medium priority by the GSAs in the KCS. It is located along the Friant-Kern Canal between Mileposts 130 and 137, southwest of Famoso and Poso Creek (**Figure 5a**). Annual subsidence rates identified by this current study is estimated at between 2 to 3 inches and are a result of agricultural activity (Figure 8). An area of higher annual rate of subsidence (minimum

of 3 inches) is located immediately to the west of AOI 3. That subsidence is also attributable to agricultural activities.

California Aqueduct Mileposts 267 to 271 (AOI 4)
This AOI was rated as medium priority by the GSAs in the KCS (**Figure 5a**). A review of the NASA/JPL rate of subsidence for 2015-2016 shows this area experienced between 2 and 4 inches of subsidence for that period (**Figure 5**). Data provided in this current study indicates an average subsidence rate for the period April 2015 to September 2020 was around 1 to 2 inches.

North Boundary of Subbasin (AOI 5)
The GSAs in the KCS identified this area as medium priority (**Figure 5a**). While there is reportedly no large critical infrastructure nearby this AOI there are many individual well casings that could be affected by localized subsidence. Coordinated monitoring with adjacent GSAs, both within the KCS, and those adjacent GSAs outside of the KCS is recommended. A review of the rate of subsidence for 2015-2016 presented in the 2020 NASA/JPL data shows this AOI reportedly experienced between 5 and 8 inches of subsidence for that period (**Figure 5**). Data provided in this current study indicates an average subsidence rate for the period April 2015 to September 2020 was around 2 to 4 inches, with isolated areas slightly higher. The cumulative subsidence for the current study period is approximately 5 to 10 inches versus 10 to 15 inches for the period 2015 to 2017 presented in the NASA/JPL data. (**Figure5**). It appears areas immediately to the north of the AOI outside of the KCS are experiencing significantly higher cumulative subsidence ranging from between 20 to 40 inches in places during this current study period.

5.0 CONCLUSIONS AND RECOMMENDATIONS

5.1 CONCLUSIONS

Based on the data and methodology presented above, we conclude the following:

- Sentinel-1 SAR data provides a viable method of mapping and monitoring subsidence within the KCS, especially when combined with a stacking method that reduces atmospheric noise and that allows the data set to be reliably calibrated against continuous GPS stations in the area.
- The vertical resolution of the DInSAR stack for this current study is approximately 2.4mm/year based on comparisons with data from KCS continuous GPS stations in the study area. The error rate is approximately 2.4mm/year (one standard deviation).
- Though subsidence rates identified in this study require careful future monitoring, we believe previous studies may be overestimating by 45 to 50% the subsidence rates associated with seasonal groundwater extraction within the KCS. This is due to the short time intervals related to the acquisition of available InSAR data (Confirmed by JPL, Personal communication with Dr. Zhen Liu, 2021).
- The northern boundary of the KCS is administrative and not hydraulically-based. Groundwater extraction activities to the north of the KCS should be considered in SGMA related planning and be included in future monitoring as these activities contribute to the subsidence in areas along the northern KCS boundary.

- Although subsidence is generally envisioned to be primarily vertical phenomenon, there is also a horizontal stress (3-dimensional) geomechanical component to subsidence that can have profound effects on infrastructure such as aqueducts, canals pipelines and well casings.

- DInSAR provides a useful and economical tool for siting ground-based monitoring technology (e.g. new GPS or extensometers) to enhance KCS coordination and monitoring efforts

- Discerning the difference between subsidence caused by seasonal (cyclical) groundwater extraction and non-seasonal; (i.e., long term) oilfield activities is possible utilizing DInSAR. The ability to ascertain these differences are enhanced when DInSAR is integrated with GPS or location-specific ground-based technology (e.g., extensometers, new GPS stations etc.).

5.2 RECOMMENDATIONS

As a result of this study, we recommend the following:

1. Conduct additional assessment of the apparent discrepancies between the current DInSAR results and NASA/JPL subsidence data, in areas subject to seasonal groundwater withdrawal by sharing the results of this current study with NASA/JPL.
2. Future InSAR studies should include a minimum time interval of five years' worth of InSAR data to enhance data resolution and accuracy.
3. The 3-dimensional forces associated with ground subsidence include horizontal stresses. These stresses can have expensive and long-term undesirable results on critical infrastructure such as the California Aqueduct and the Friant-Kern Canal within the KCS. The scientists at the Lawrence-Berkeley Laboratory (LBL) have demonstrated expertise in assessing the effects of vertical and horizontal geo-mechanical stress on infrastructure. It is recommended that the KCS consider engaging LBL to conduct a geo-mechanical (horizontal stress) assessment of the five AOIs with an emphasis on the critical water infrastructure (e.g., the California Aqueduct and Friant-Kern Canal).
4. LBL study partners for the purpose of cost sharing could include the DWR and Friant Water Authority, respectively. The results of the study could have significant implications on proposed or planned infrastructure rehabilitation projects, including their effectiveness, permanence, and cost.
5. Conduct a detailed analysis of the current DInSAR data and existing (2020) KCS hydrogeologic data (e.g. groundwater quality, groundwater levels and groundwater flow modeling etc.) to further refine the potential nexus between oil field activities and undesirable results to critical infrastructure in the KCS.
6. Continue coordination efforts with GSs to the north of the KCs with a focus on subsidence monitoring and reporting.

6.0 REFERENCES CITED

Amelung, F., Galloway, D.L., Bell, J.W., Zebker, H.A., and Laczniak, R.J, 1999**,** Sensing the ups and downs of Las Vegas: InSAR reveals structural control of land subsidence and aquifer-system deformation: *Geology*, Vol. 27, pp. 483–486.

Aquilogic, Inc., 2019, Chapter Groundwater Sustainability Plan Westside District Water Authority Kern County, California

Aquilogic, Inc., 2020, PowerPoint Presentation, Draft WDWA Subsidence review, presented to the Westside District Water Authority Kern County, California

Bawden, G.W., 2003, Separating groundwater and hydrocarbon-induced surface deformation from geodetic tectonic contraction measurements across metropolitan Los Angeles, California; *In* Prince, K.R. and Galloway, D.L., (editors), *Proceedings of the Subsidence Interest Group Conference Technical Meeting* held in Galveston, Texas, November 27-29, 2001: U.S. Geological Survey Open-File Report 03-308; available from http://pubs.usgs.gov/of/2003/ofr03-308/.

Borchers, J.W., Carpenter, M., Kretsinger-Grabert, V., Dalgish, B., and Cannon, D., 2014, Land Subsidence from Groundwater Use in California: Water Education Foundation and Luhdorff & Scalmanini Consulting Engineers, 161p.

California Department of Water Resources (CDWR), 2015, Sustainable Groundwater Management Program Draft Strategic Plan, 31p.

California Department of Water Resources (CDWR), 2020, SGMA Groundwater Management, https://water.ca.gov/Programs/Groundwater-Management/SGMA-Groundwater-Management

Farr, T., Jones, C.E., Liu, Z., 2017, Jet Propulsion Laboratory, California Institute of Technology, Progress Report: Subsidence in California, March 2015 – September 2016

Galloway, D.L. and Burbey, T.J., 2011, Review: Regional land subsidence accompanying groundwater extraction: *Hydrogeology Journal, Vol.* 19, No. 8: pp. 1459-1486.

GEI Consultants, Inc., January 2020, Kern Groundwater Authority Groundwater Sustainability Plan

Hu, J., Ding, X.L., Lia, Z.W., Zhang, L., Zhu, J.J., Sun, Q., and Gao, G.J., 2016, Vertical and horizontal displacements of Los Angeles from InSAR and GPS time series analysis: Resolving tectonic and anthropogenic motions: *Journal of Geodynamics*, Vol. 99, Sept 2016, pp. 27-38.

Lanari R., Lundgren P., Mariarosaria M., and Casu, F., 2004, Satellite radar interferometry time-series analysis of surface deformation for Los Angeles, California: *Geophysical Research Letters,* Vol. 31, No. 23, 16 Dec. 2004, 5p.

Orange County Water District, 2015, Groundwater Management Plan 2015 Update, 10p.

Poland, J.F., (editor), 1984, Guidebook to Studies of Land Subsidence due to Ground-water Withdrawal: *Studies and Reports in Hydrology*, prepared for the International Hydrological Programme, Working Group 8.4: United Nations Educational, Scientific and Cultural Organization, Paris, France, 305p. plus Appendices; available from http://unesdoc.unesco.org/images/0006/000651/065167eo.pdf

Sneed, M., 2016, Land Subsidence: The Lowdown on the Drawdown: US Geological Survey and California Groundwater Resources Association Webinar, March 23, 2016.

Towill, Inc., 2020, InSAR Data Accuracy for California Groundwater Basins, CGPS Data Comparative Analysis January 2015 to September 2019, March 23, 2020.

TRE Altamira, Inc., 2020, InSAR land surveying and mapping services in support of the DWR SGMA program, Technical Report, 16 March 2020